Available online at www.sciencedirect.com
SciVerse ScienceDirect
www.elsevier.com/locate/jmbbm

Research Paper

Mechanical properties and *in vitro* evaluation of bioactivity and degradation of dexamethasone-releasing poly-D-L-lactide/nano-hydroxyapatite composite scaffolds

Ling Chen[a], *Chak Yin Tang*[a,*], *Chi Pong Tsui*[a], *Da Zhu Chen*[b]

[a]*Department of Industrial and Systems Engineering, The Hong Kong Polytechnic University, Hung Hom, Kowloon, Hong Kong, China*
[b]*College of Materials Science and Engineering, Shenzhen University, Shenzhen, Guangdong, China*

ARTICLE INFO

Article history:
Received 10 December 2012
Received in revised form
15 March 2013
Accepted 17 March 2013
Available online 2 April 2013

Keywords:
PDLLA/nano-HAp composites
In vitro bioactivity
Mechanical properties
Biodegradation
Drug releasing

ABSTRACT

The purpose of this study was to fabricate drug-release nano-composite scaffolds and perform *in vitro* evaluation of their mechanical properties, bioactivity, biodegradability and drug release behaviors. Porous drug-release poly-D-L-lactide (PDLLA) composite scaffolds filled with different amounts of nano-hydroxyapatite (nano-HAp) were prepared by a technique combining polymer coagulation, cold compression moulding, salt leaching and drug coating. Apatite detected on the scaffolds after exposure to a simulated body fluid showed improvement in bioactivity and the apatite formation ability through the addition of the nano-HAp content in the composites. Nano-HAp incorporation and apatite formation made a positive impact on the mechanical properties of the scaffolds; however, plasticization and degradation of PDLLA had a negative impact. The pH-compensation effect of the composite scaffolds can reduce the risk of chronic inflammation complications. The fabrication method in this study can produce scaffolds with controllable structure, appropriate mechanical properties and degradation rates for cancellous bone repair applications.

1. Introduction

Biodegradable polymer/inorganic particle composites with drug delivery functions have attracted increasing attention as promising candidates for bone tissue scaffolding (Mourino and Boccaccini, 2010). Compared to biodegradable polymers (*e.g.* poly(ε-caprolactone) (PCL), poly(lactic acid) (PLA), poly (glycolic acid) (PGA), and their copolymer poly(DL-lactic-co-glycolic acid) (PLGA)) or the inorganic particles (*e.g.* hydroxyapatite (HAp), calcium phosphate (BCP, TCP), and Bioglass®), composites combining the advantages of both polymers and inorganic particles have high mechanical performance and attractive bioactive properties (Armentano et al., 2010). These composite scaffolds play an important role in bone tissue engineering as templates for cell attachment, proliferation, differentiation, and the formation of bone-extracellular matrices (ECM). The composite scaffolds can not only provide structural support for the newly formed tissue (Hutmacher, 2001; Karageorgiou and Kaplan, 2005; Liu et al., 2007), but also act as drug carriers to deliver biologically active molecules at a desired rate for an appropriate period of treatment, which may reduce side effects and optimize drug

*Corresponding author. Tel.: +852 2766 6608; fax: +852 2362 5267.
E-mail address: mfcytang@inet.polyu.edu.hk (C.Y. Tang).

1751-6161/$ - see front matter © 2013 Elsevier Ltd. All rights reserved.
http://dx.doi.org/10.1016/j.jmbbm.2013.03.008

administration, thereby improving the therapeutic efficiency and safety of drugs (Langer, 1998). Biodegradable poly-D,L-Lactide/nano-hydroxyapatite (PDLLA/nano-HAp) composites have been increasingly studied for bone regeneration (Zheng et al., 2006; Chen et al., 2011). The mechanical properties and the hydrophilicity of these nano-composites can be effectively improved when nano-HAp is incorporated into the polymer (Chen et al., 2011). Moreover, such nano-composites have shown improved osteoconductivity and bioactivity, partially due to the enhanced bonding between the composites and bone.

Degradation behavior of composite bone scaffolds is of crucial importance in tissue engineering, because the degradation rate is essentially linked to cell growth, host response and tissue regeneration (Babensee et al., 1998). Ideally, the scaffolds should have a degradation rate that matches the regeneration rate of new bone tissue. The degradation kinetics of composite scaffolds can be affected by their microstructure, chemical and physical properties, molecular weight as well as environmental conditions (Wu and Ding, 2004; Söntjens et al., 2012). Therefore, control and evaluation of the degradation behavior of composite scaffolds are important for the success of a biodegradable scaffold for bone tissue engineering.

In vitro test is usually done before *in vivo* test, because it is cheaper and less time consuming, and *in vivo* test has a lot of restrictions. Kokubo (1991) suggested that the deposition of a bonelike apatite layer on the surface of an artificial biomaterial is the essential requirement for bonding to living bone. His group firstly reported that apatite deposition in a simulated body fluid (SBF) could be reproduced when the artificial biomaterial was implanted in a living body (Oyane et al., 2003). This means that a SBF, with nearly the same ion concentrations as human blood plasma, can be applied to estimate *in vitro* bioactivity of the material from the apatite formation on the implant surface. In addition to the *in vitro* bioactivity assessment, soaking in a SBF to form a biomimetic apatite coating on artificial biomaterials has recently become a strategy to improve the biological properties of materials (Tanahashi et al., 1994; Song et al., 2004). Since the biomimetic apatite formation on an implant material surface has been described as beneficial for cell response, the majority of research studies have focused on the mechanism and time requirement for apatite formation in a SBF, as well as modification to the formulation or pH value of a SBF for accelerating apatite formation (Chou et al., 2004; Chen et al., 2005). Recently, effects of SBF incubation on mechanical properties of bioactive scaffolds (*e.g.* PDLLA/Bioglass® bone scaffolds and 13-93 bioactive glass porous constructs) have been investigated (Blaker et al., 2011; Kolan et al., 2012). However, very limited studies have been reported on the changes of the mechanical properties of biodegradable porous PDLLA/nano-HAp composite scaffolds during incubation in a SBF.

In our previous work (Chen et al., 2011), a novel method combining polymer coagulation, cold compression molding and particulate leaching was developed for fabricating dexamethasone (Dex)-release PDLLA/nano-HAp scaffolds, with controllable pore size and porosity. The improved wettability and mechanical properties of the PDLLA/nano-HAp composite scaffolds without incubation in simulated body fluids were well confirmed. The effects of porosity and nano-HAp addition on the Dex release profiles of the PDLLA scaffolds were also investigated. Higher Dex release amounts from the PDLLA scaffolds with larger porosity and more nano-HAp content were achieved. In this study, *in vitro* evaluation of the bioactivity, degradability, and mechanical properties of porous polyethylene glycol (PEG)/Dex coated PDLLA scaffolds, with different amounts of nano-HAp, was undertaken. The bioactivity of the scaffolds was validated from the bonelike apatite deposition on the surface of the scaffolds after incubation in a SBF. The relationship between the SBF immersion time and the compressive modulus and strength of the PDLLA/nano-HAp scaffolds was monitored in detail. In addition, the morphology, molecular weight and mass changes of the scaffolds, as well as the pH value of the phosphate buffered saline solution (PBS, pH 7.4), were investigated. A drug release study was also carried out to find out the influence of the incorporated nano-HAp amount on the drug release behavior of the composite scaffolds. The correlations between the mechanical properties change and drug release rate of the PDLLA/nano-HAp composite scaffolds, and their degradation process, are very significant for better understanding and efficient prediction of scaffold degradation, so that improved scaffolds for tissue engineering applications can be designed.

2. Materials and methods

2.1. Materials

PDLLA ($\overline{M_\eta} = 75,000$) was supplied by the Jinan Daigang Bio-Technology Co., Ltd. (China). Nano-HAp particles (20–30 nm) were purchased from the Berkeley Advanced Biomaterials, Inc. (USA). Dex (CAS 50-02-2, 98% purity), the drug model, was purchased from the Sigma Aldrich Co., Ltd. PEG ($\overline{M_w} = 6000$) and sodium chloride (NaCl) supplied by the Tianjin Reagent Chemical Co., Ltd. (China). Chloroform was purchased from the Shanghai Shenxiang Chemical Reagent Co., Ltd. (China). All chemicals and reagents were of analytical grade and used without further purification.

2.2. Fabrication of porous PDLLA/nano-HAp scaffolds with PEG/Dex coating

The PEG/Dex coated porous PDLLA scaffolds filled with different amounts of nano-HAp (0, 20, 40 and 60 wt%) were fabricated using the techniques developed in our previous work (Chen et al., 2011). The PDLLA/nano-HAp scaffolds with a porosity of around 80% were produced by controlling the weight ratio of PDLLA and NaCl to 1:8. The PDLLA was firstly dissolved in chloroform, and nano-HAp and sieved NaCl particles (150–300 μm) were subsequently dispersed in the PDLLA/chloroform solution by a homogenizer. PDLLA/NaCl/nano-HAp gel paste was precipitated by dropping ethanol into the solution. This gel paste was then compression molded into a specimen with dimensions of 10 mm in diameter and 5 mm in height using a powder compressing machine (Model 769YP-15A) under 10 MPa at room temperature. After salt leaching and drying of the molded composites,

porous PDLLA/nano-HAp scaffolds were prepared. Finally, PEG/Dex coated porous scaffolds were fabricated by immersing the pre-prepared PDLLA/nano-HAp porous scaffolds in a hydrophilic PEG/Dex (20/0.8, w/w) solution (10 ml) under vacuum for 24 h. The total drug loading amounts were determined by using a UV/vis spectrophotometer.

2.3. *In vitro evaluation of the bioactivity of porous PDLLA/nano-HAp scaffolds*

2.3.1. *Soaking in a SBF*

The bioactivity of a material can be evaluated by examining the apatite forming ability on its surface in a SBF which contains similar ion concentrations to those present in human blood plasma. To prepare 1000 ml of the SBF solution, reagent grade chemicals, NaCl (8.035 g), $NaHCO_3$ (0.355 g), KCl (0.225 g), $K_2HPO_4 \cdot 3H_2O$ (0.231 g), $MgCl \cdot 6H_2O$ (0.311 g), 1.0 M-HCl (39 ml), $CaCl_2$ (0.292 g), Na_2SO_4 (0.072 g), and Tris (6.118 g) were dissolved into deionized water one by one in this order and buffered with 1.0 M-HCl to pH 7.4 at 37 °C under stirring (Kokubo and Takadama, 2006).

The unfilled PDLLA scaffolds and the scaffolds with different amounts of nano-HAp were immersed separately in clean plastic flasks with the SBF. Lids were placed on the flasks to form an airtight seal for preventing contamination. The scaffolds were soaked in the SBF at 37 °C without vibration for 7 days, 14 days, and 28 days. The mediums were refreshed every 7 days. After the various soaking periods, the samples were then taken out from the flasks, washed gently with deionized water and then vacuum dried overnight at 40 °C.

2.3.2. *Morphology observation and elemental analysis*

The microstructure changes and the morphology of the deposited biomimetic apatite layer on the scaffold surfaces after incubation in the SBF were characterized using scanning electron microscopy (SEM, JEOL JSM-6490). The polymeric samples were coated with gold to improve their conductivity. The elemental composition of the surface apatite layer on the scaffolds was examined by an energy dispersive X-ray analysis detector (EDX, Oxford, INCA 250 Energy System).

2.3.3. *X-ray diffraction (XRD) characterizations*

The phase structures of the unfilled PDLLA, PDLLA/nano-HAp and the PDLLA/nano-HAp scaffolds after soaking in SBF for 28 days were characterized by an X-ray diffractometer (XRD, Bruker D8 Discover) with Cu K_α radiation. The samples were scanned at 2-*theta* angles, ranging from 10° to 50°, at a scanning rate of 0.02 °/s.

2.4. *Molecular weight determination*

Molecular weight changes of the scaffolds with different nano-HAp amounts were determined by using a gel permeation chromatography (GPC, Waters Associates, Inc.) system. The measurements were carried out at 30 °C and at a flow rate of 1 ml/min using tetrahydrofuran (THF) as an eluent. A set of monodisperse linear polystyrene standards (Polysciences, Inc.) was used to obtain a calibration curve. The weight average ($\overline{M_w}$) molecular weights of the scaffolds were estimated. Three replicate measurements were conducted for each type of sample.

2.5. *Weight loss*

The original mass of the unfilled PDLLA and PDLLA/nano-HAp scaffolds was measured prior to incubation in the SBF. After the samples had been soaked in the SBF for different time periods, they were dried for 24 h in a vacuum oven at room temperature, and weighed again. The weight loss (W_L) of each sample was obtained from

$$W_L = (W_O - W_D)/W_O \times 100\% \quad (1)$$

where W_O is the original mass of the scaffold, and W_D is the dry weight of the scaffold measured after each incubation period. Three scaffold specimens were measured for each type of the sample.

2.6. *Mechanical behavior characterization*

In order to investigate how apatite formation and scaffold degradation affect the mechanical properties of the unfilled PDLLA and PDLLA/nano-HAp scaffolds, uniaxial compression tests were carried out at room temperature using a mechanical universal testing machine (MTS 810, Material Test System). The compressive moduli and strengths of the cylindrical samples, before and after incubation for different periods in the SBF (*i.e.* 0 days, 7 days, 14 days and 28 days) were determined. A crosshead speed of 2 mm/min and a load cell of 500 N were adopted for the tests. The compressive modulus (E) and the strength (σ_{10}) of each sample were determined by measuring the slope of the initial linear portion of the stress–strain curve and the stress at which the strain reached 10%, respectively (ASTM standard, D1621). Five specimens were examined for each type of scaffold sample.

2.7. *Drug release studies and pH value changes*

The PEG/Dex coated scaffolds, with different amounts of nano-HAp, were separately placed in closed vials with 10 ml of 10 mM PBS. These vials were placed in a water bath at 37 °C for 35 days to allow drug release from the scaffolds. Each medium with the released Dex was collected at specific time intervals and replaced with an equal amount of new PBS. The time of collecting and replacing the PBS medium followed the sequence of 1, 2, 3, 5 and 10 h and then 1, 2, 3, 5, 7, 10, 15, 20, 25, 30 and 35 days. The mediums were analyzed by a UV/vis spectrophotometer (UV1102, Techcomp Ltd.) at a wavelength of 242.5 nm, while the pH values of the PBS mediums were recorded using a pH meter (SevenGo™ pH-SG2, Mettler Toledo).

2.8. *Statistical analysis*

One-way analysis of variance (ANOVA) was performed for every assay and the results were expressed as mean ± standard deviations. A Fisher's least significant difference (LSD) test was used to compare between the sample means, and determine the statistical significance of the data for $p < 0.05$.

3. Results and discussions

3.1. *In vitro bioactivity studies*

3.1.1. *Microstructure changes of the scaffolds*

Fig. 1 shows the SEM images of the unfilled scaffolds and the 60 wt% nano-HAp filled PDLLA scaffolds prior to incubation in the SBF. The homogeneous pore distribution in the scaffolds is clearly observed. The average pore size of the scaffolds shown in Fig. 1, determined by the size of the porogen, NaCl particles, is around 250 μm, which meets the requirement of a bone scaffold for promoting new bone regeneration and vascularization (Karageorgiou and Kaplan, 2005). The nano-HAp filled PDLLA scaffolds have a rougher pore wall surface compared to the unfilled ones, because some of the nano-HAp are located on the surface of the scaffolds, as shown in Fig. 1. Moreover, the dispersion of nano-HAp in the PDLLA matrix has been found to be homogenous by EDX analysis (Chen et al., 2011).

The microstructure changes of the PDLLA composite scaffolds (filled with 0 wt%, 20 wt%, 40 wt% and 60 wt% of nano-HAp) after incubation in the SBF for 7 and 28 days are shown in Fig. 2. For the unfilled PDLLA scaffolds after 7-day incubation, as shown in Fig. 2(a), the pore walls become thinner and the pore sizes obviously increase, as compared with Fig. 1(a). For the nano-HAp filled scaffolds, Fig. 2(b–d) shows a relatively smaller increase in pore sizes compared with the unfilled one after 7-day incubation, as shown in Fig. 2(a). Moreover, from the high-magnification SEM images of the PDLLA composite scaffolds after 7-day incubation (Fig. 2(a–d)), apparently some apatite crystals are deposited on all types of scaffolds and the amount of the deposited apatite increases with increasing nano-HAp amount in the scaffolds. Moreover, more apatite can be observed on the surface of the PDLLA/nano-HAp scaffolds than the unfilled ones for the same incubation time. After 28-day immersion in the SBF, all the PDLLA based scaffolds show larger pore sizes and their pore surfaces are covered with a layer of apatite, as shown in Fig. 2 (e-h). The amount of the apatite deposition increases with the incubation time. A few flake-like apatite particles were formed on the surface of the scaffolds after incubation for 7 days, while more and bigger apatite particles were formed and joined together on the scaffolds after 28-day incubation. The deposited apatite particles almost form a continuous layer on the PDLLA scaffold with 40 wt% of nano-HAp as shown in Fig. 2(g), and some additional particles are deposited on the former apatite layer on the scaffold filled with 60 wt% of nano-HAp after 28 days of incubation as shown in Fig. 2(h). The results suggest that PDLLA scaffolds, containing more nano-HAp, can facilitate the formation of biological apatite. This finding is in agreement with some previous studies where the addition of nano-HAp not only acted as a reinforcing filler, but also provided a bioactive property to the composites (Chen et al., 2007; Deng et al., 2008).

An EDX analysis was conducted to confirm the presence of apatite grown on the surface of the composite scaffold after incubation. As the filled weight fraction of the nano-HAp does not significantly affect the atomic components of calcium phosphate (Deplaine et al., 2010), and the surface of the PDLLA composite scaffold with 60 wt% of nano-HAp was fully covered with apatite after a 28-day incubation in the SBF, as shown in Fig. 2(h), this sample was therefore chosen as the representing sample for the EDX test. An EDX spectrum of the apatite grown on the surface of the PDLLA/60 wt% nano-HAp composite scaffold (as the result of the representative volume) is illustrated in Fig. 3, where the main elements of the surface mineral layer were C, O, P, and Ca, and the Ca/P ratio of 1.59, confirming the presence of calcium-deficient and non-stoichiometric apatite on the surface of the scaffold after incubation. It is known that natural bone is lower than 1.67 when compared to stoichiometric apatite; therefore, the apatite formed on the scaffolds is of greater biological interest than the stoichiometric apatite, from the view of biomemetics (Deng et al., 2001).

3.1.2. *XRD characterizations*

The thin-film X-ray diffraction (TF-XRD) patterns of the PDLLA scaffolds, with and without nano-HAp, before and after incubation in the SBF for 28 days, are shown in Fig. 4. The unfilled amorphous PDLLA matrix is characterized by the broad 2θ peaks between 10° and 25°, as shown in Fig. 4(a). The characteristic peaks of HAp observed in Fig. 4(b) confirm the successful incorporation of the nano-HAp into the PDLLA scaffolds. After 28-day immersion in the SBF, the PDLLA/nano-HAp scaffolds show characteristic peaks at $2\theta = 25.8°$,

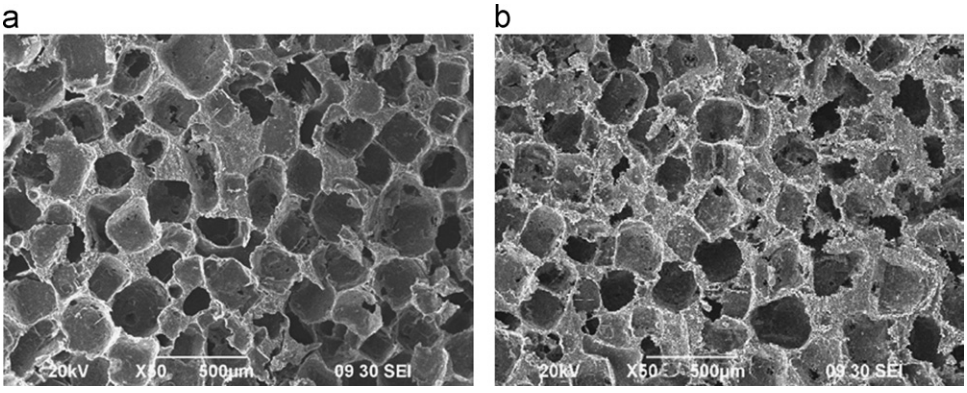

Fig. 1 – SEM micrographs of porous scaffolds before incubation in SBF: (a) unfilled PDLLA and (b) PDLLA filled with 60 wt% of nano-HAp.

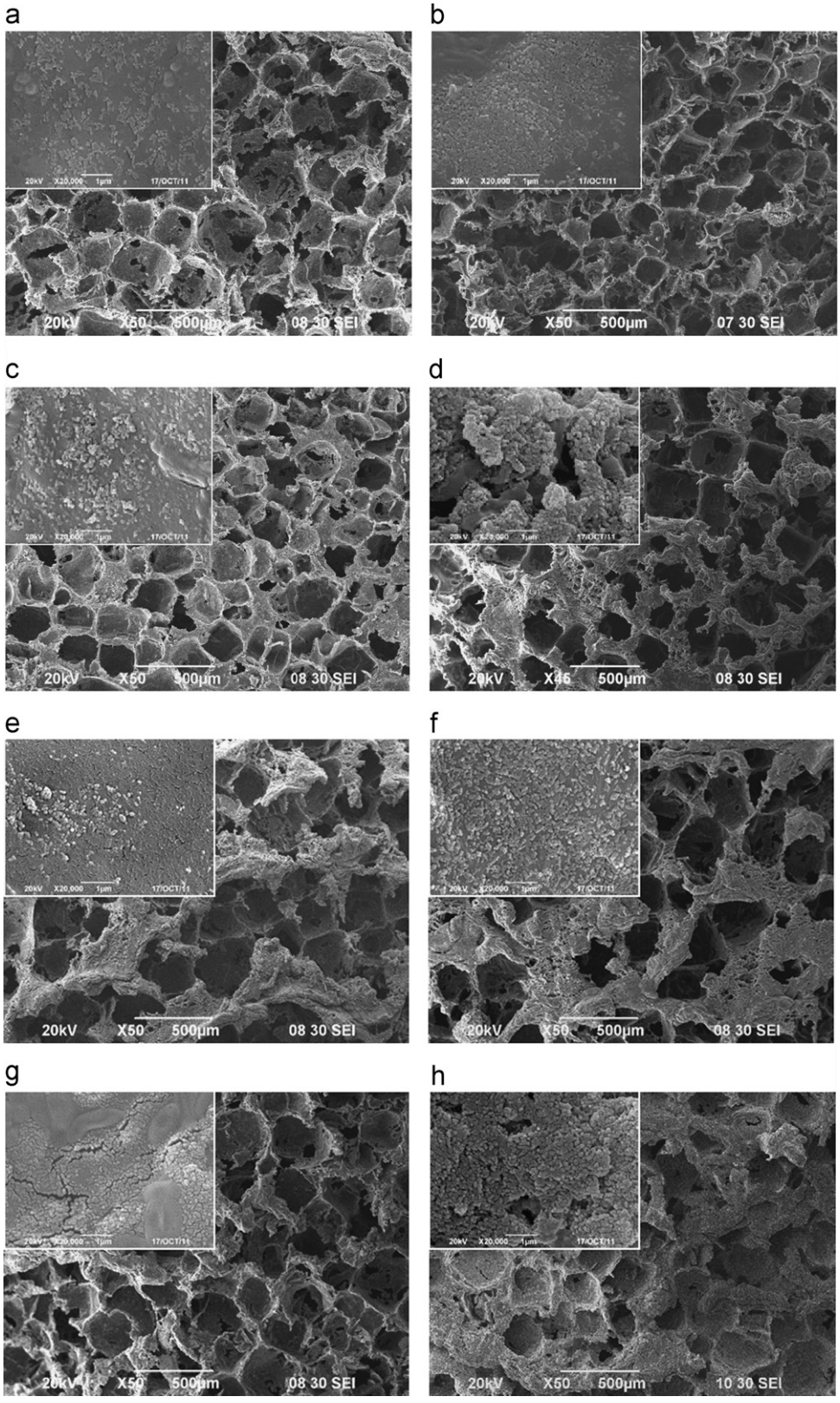

Fig. 2 – SEM micrographs of porous scaffolds after incubation in SBF for (a–d) 7 days and (e–h) 28 days at low and high magnification: (a, e) unfilled PDLLA, PDLLA filled with (b, f) 20 wt%, (c, g) 40 wt%, and (d, h) 60 wt% of nano-HAp.

31.7°, 32.9° and 46.7°, which correspond to the formed Ca–P crystal layer as shown in Fig. 4(c). The peaks for the scaffolds after incubation in the SBF are stronger and broader than those prior to incubation. This further confirms the formation of the Ca–P crystal layer on the PDLLA/nano-HAp scaffolds after incubation in the SBF.

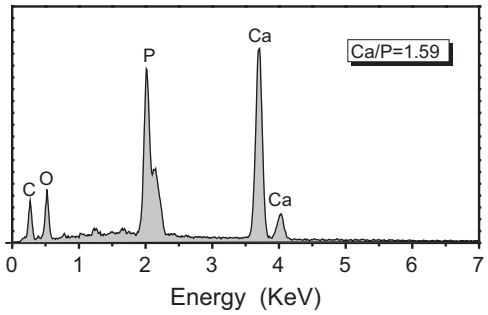

Fig. 3 – EDX spectrum for confirming the presence of apatite formation on the surface of the PDLLA/60 wt% nano-HAp composite scaffold after incubation in SBF at 37 °C for 28 days.

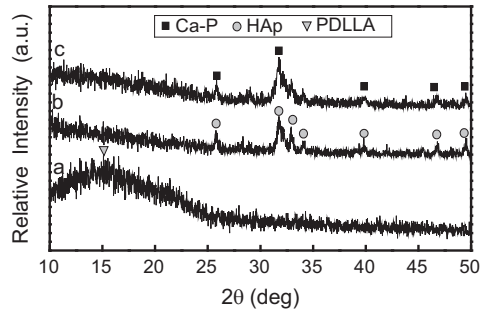

Fig. 4 – TF-XRD graphs of (a) unfilled PDLLA scaffold before immersion in SBF; (b) PDLLA/60 wt% nano-HAp scaffold before immersion in SBF; and (c) PDLLA/60 wt% nano-HAp scaffold after immersion in SBF for 28 days.

3.2. *The change of molecular weight and mass of the scaffold*

The weight average molecular weights ($\overline{M_w}$) of PDLLA for the different kinds of the scaffolds fabricated in this study were measured by gel permeation chromatography (GPC) and are shown in Fig. 5. From Fig. 5, the $\overline{M_w}$ of the PDLLA for all the scaffolds, with and without nano-HAp addition, decreases with time after incubation in the SBF, resulting from the degradation of the PDLLA polymer. After a 28-day incubation, the unfilled PDLLA scaffold has the lowest $\overline{M_w}$ compared to the filled ones. However, for the first 7-day incubation, the degradation rate increased when the PDLLA scaffolds were filled with larger amounts of nano-HAp, because the PDLLA scaffolds with higher nano-HAp content could increase the hydrophilicity of the scaffolds and hence promote the penetration rate of the SBF. Therefore, the $\overline{M_w}$ of the PDLLA scaffolds with 60 wt% of nano-HAp decreases faster than other filled scaffolds, as shown in Fig. 5. In all, incorporation of the nano-HAp can be used to control the degradation rate of the PDLLA/nano-HAp scaffolds.

Fig. 6 shows the weight losses of the scaffolds during the first 28-day incubation in the SBF. The weight losses of all the PDLLA scaffolds immersed in SBF increase with time. It can be observed from Fig. 6 that the weight losses of the scaffolds with 20 wt%, 40 wt% and 60 wt% of nano-HAp after 28 days of incubation are 1.9%, 2.2% and 4.2%, respectively.

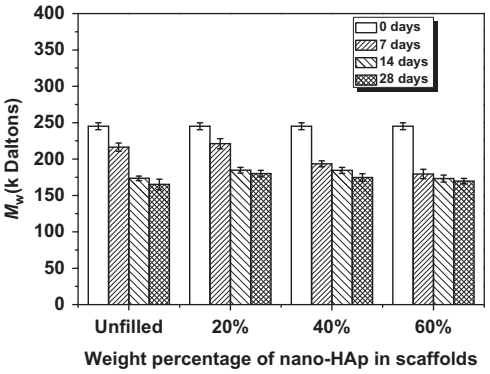

Fig. 5 – Weight average molecular weight (Mw) changes of PDLLA scaffolds with 0, 20, 40, 60 wt% of nano-HAp after incubation in SBF for different time periods. Results are mean ± SD. *, #, And & indicate statistically significant difference as compared with 0 day, 7 days, and 14 days, respectively ($n=3$, $p<0.05$).

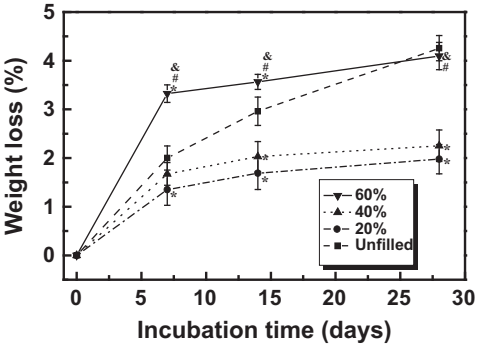

Fig. 6 – Weight losses of the PDLLA scaffolds filled with different amounts of nano-HAp (0, 20, 40, and 60 wt%) after incubation in SBF for different time periods. Results are mean ± SD. *, # And & indicate statistically significant difference as compared with unfilled scaffold, 20 wt% and 40 wt% nano-HAp filled PDLLA scaffolds, respectively ($n=3$, $p<0.05$).

This suggests that the PDLLA scaffolds with 60 wt% of nano-HAp have the highest weight losses during their incubation in the SBF for 28 days as compared with others. However, there is no statistically significant difference in the weight losses between the scaffolds with 20 wt% and 40 wt% of nano-HAp during the incubation period. The rapid weight losses of the composite scaffolds are probably due to the dissolution of the nano-HAp particle, degradation and fragmentation of the polymer matrices in the scaffolds. On the other hand, nano-HAp incorporation increases the overall hydrophilicity of the scaffolds which results in increasing their hydrolysis rates. Therefore, the scaffolds with high amounts of nano-HAp, for example, 60 wt%, have a faster weight loss rate especially during the first 7-day incubation (Ang et al., 2006). However, the weight loss of the unfilled scaffold is higher than that of the scaffolds with 20 wt% and 40 wt% of nano-HAp but lower than that of the scaffold with 60 wt% after 7 days. It is because the higher amounts of apatite deposition on the

scaffolds with 20 wt% and 40 wt% of nano-HAp than that of the unfilled one can retard the weight loss of the composite scaffolds. As the apatite deposition rates of the unfilled PDLLA scaffolds are slower than the PDLLA/nano-HAp ones during incubation in the SBF, the unfilled PDLLA scaffolds have a higher weight loss of nearly 4.4% after 28-day immersion, as compared with the filled ones. However, the weight loss difference between the unfilled scaffold and the scaffold with 60 wt% of nano-HAp after 28-day immersion is not statistically significant.

3.3. *Mechanical properties evolution of the scaffolds*

3.3.1. *Before SBF incubation*

The compressive moduli (E) and strengths (σ_{10}) of the PDLLA scaffolds with different amounts of nano-HAp before incubation in the SBF are shown in Fig. 7, noted as 0-day incubation. Before incubation, PDLLA/nano-HAp scaffolds have higher compressive moduli and strengths than the unfilled PDLLA ones. E and σ_{10} of the PDLLA with 60 wt% of nano-HAp increased to 91.3 ± 1.2 MPa and 2.5 ± 0.2 MPa, respectively, which are close to the data for human cancellous bone (Rezwan et al., 2006). The increase in E for the PDLLA/nano-HAp scaffolds is mainly attributed to the addition of the rigid nano-HAp filler (Thomas et al., 2006). HAp in nano size with a high total surface area can enhance stress transfer between the matrix and the fillers. Therefore, the addition of nano-HAp led to the increase in σ_{10} through an efficient stress transfer mechanism (Fu et al., 2008). In addition to the high surface area of the nano-HAp, the interfacial adhesion between the fillers and the polymer matrix is of crucial importance for compressive strength (Kovačevic et al., 2008). The hydrogen bonding formed between the uniformly distributed nano-HAp and the PDLLA matrix under compression molding also increased the interfacial adhesion and hence the enhancement of compressive strength of the PDLLA/nano-HAp composites is due to the better load transfer (Zhou et al., 2007; Fu et al., 2008).

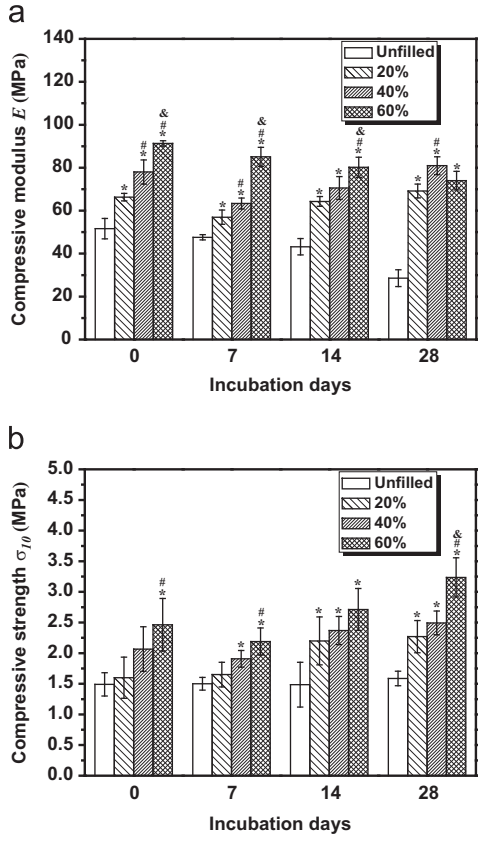

Fig. 7 – (a) Changes in compressive moduli (E) and (b) strengths (σ_{10}) of the PDLLA scaffolds with different amounts of nano-HAp after incubation in SBF for different time. Results are mean $\pm$ SD. *, #, And & indicate statistically significant difference as compared with unfilled PDLLA, PDLLA with 20 wt% and 40 wt% of nano-HAp, respectively ($n=5$, $p<0.05$).

3.3.2. *After SBF incubation*

The changes of compressive moduli and strengths of the unfilled PDLLA scaffolds and scaffolds with 20 wt%, 40 wt% and 60 wt% of nano-HAp after incubation in the SBF for different times are shown in Fig. 7. After soaking in the SBF for 7 days, the E values of all the PDLLA based scaffolds decrease as shown in Fig. 7(a). The main reason of this decrease is the pore size increase of the scaffolds as shown in Fig. 2, the decrease in the molecular weight of the PDLLA as shown in Fig. 5 and the loss of the nano-HAp particles. In addition, the reduction of E can also be attributed to the plasticizing effect because the terminal carboxylic acid functional group on the PDLLA chains facilitates water penetration (Blaker et al., 2011). From the 7-day to 28-day incubation, it can be observed that the E values of the PDLLA scaffolds with 20 wt% and 40 wt% of nano-HAp increase with incubation time. The increase of E can be mainly attributed to the apatite deposition on the scaffolds and the improvement of the interfacial adhesion between the deposited apatite and the PDLLA matrix. From Fig. 7(a), the E of the unfilled PDLLA scaffolds reduces from 51.6 ± 4.7 MPa to 28.6 ± 3.9 MPa after a 28-day incubation, because of the continuous degradation of the PDLLA and the relatively little apatite being deposited during the incubation. Nano-HAp particles filled in the PDLLA scaffold tended to fall off and interact with the SBF because of their good hydrophilicity. The loss of nano-HAp particles leads to the formation of some voids within the PDLLA matrix, and hence more surfaces of the PDLLA are exposed to hydrolytic attack, accelerating the degradation of the PDLLA and weakening its overall structure. Therefore, when the PDLLA scaffold is filled with higher content of hydrophilic nano-HAp, this phenomenon is more obvious and results in the E reduction of the scaffolds with 60 wt% of nano-HAp, within the 28-day incubation. However, the scaffolds with 40 wt% nano-HAp after a 28-day incubation can reach an E value of 80.9 ± 4.1 MPa, which is much larger than that of an unfilled PDLLA scaffold. In all, the incorporation of the nano-HAp into the PDLLA can promote apatite deposition on the scaffolds and enhance their compressive moduli.

On the other hand, the compressive strengths of the PDLLA based scaffolds after incubation exhibit different trends, as shown in Fig. 7(b). For the unfilled PDLLA scaffolds, σ_{10} almost maintains the same value during the incubation. σ_{10} of the PDLLA/nano-HAp composite scaffolds slightly decreases after a 7-day incubation, increases in the following

two weeks, and reaches the highest values after a 28-day incubation. In addition to the plasticization of the PDLLA matrix and the loss of the nano-HAp particles, the initial reduction of σ_{10} is mainly due to the degradation of PDLLA which increases the pore size in the scaffolds as shown in Fig. 2. With the increasing incubation time, more apatite mineral can be deposited onto the scaffold surface, leading to higher σ_{10} values for the scaffolds, especially those with high nano-HAp content. This trend is similar to that of *E*. These results endorse the importance of determining mechanical properties of PDLLA/nano-HAp scaffolds *in vitro*, because these properties are affected by the properties of the fillers, the incubation time, plasticization and degradation of the polymer.

3.4. *Drug release kinetics and the change of pH value*

The PEG/Dex coating endowed the PDLLA based scaffolds with a drug release function. An initial drug release burst is a common phenomenon for this kind of scaffold (Wang et al., 2002; Feng et al., 2010). The cumulative Dex-release curves of the PDLLA scaffolds with 0, 20, 40, and 60 wt% of nano-HAp are shown in Fig. 8. It can be seen that the Dex-release profiles of these scaffolds involve two release stages: (I) an initial burst stage (high drug release rate, in the first 10 h), and (II) a slow release stage (in the following 790 h). The occurrence of the initial burst stage is due to the free drug located near the surface of the drug coated layer (Zhang et al., 2008). After the burst, the drug slowly diffused out of the scaffolds into the PBS through some twisty pore channels in the scaffolds, over a period of 790 h (Sohier et al., 2003). Fig. 8 also illustrates that PDLLA scaffolds with a higher content of nano-HAp have a faster Dex release rate during the first 30 h. Afterwards, all the scaffolds have nearly the same release rates. This can be attributed to hydrophilic nano-HAp incorporation which improves the drug loading capacity of the scaffolds as shown in Table 1. The more the nano-HAp is filled, the thicker the PEG/Dex layer is coated on the scaffolds and the more the Dex is loaded into the scaffolds (Table 1). It is reasonable to think that the drug release rates of the scaffolds with higher concentration of the nano-HAp are higher. However, incorporating the nano-HAp fillers in the scaffolds evidently cannot affect the drug release rate as shown in Fig. 8, because the drug release rate cannot be effectively controlled only by changing the amount of the nano-HAp. Hence, other strategies, like adjustment of the pore size and porosity level of the scaffolds, should be used for controlling the drug release behavior (Chen et al., 2011).

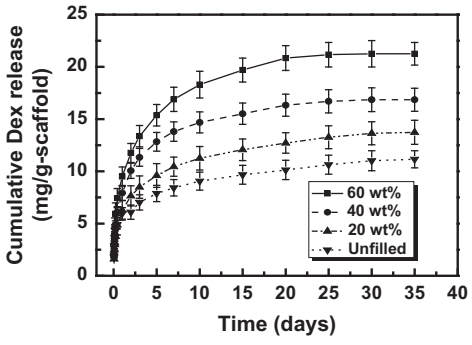

Fig. 8 – The cumulative Dex-release curves of the PDLLA/nano-HAp scaffolds with different amounts of nano-HAp (0, 20, 40, and 60 wt%). Results are mean ± SD.

Table 1 – Total drug loading amounts of the fabricated PDLLA scaffold and PDLLA/nano-HAp composite scaffolds.

Samples (PDLLA/salt, w/w)	Drug loading amounts (mg)
1:8	1.67 ± 0.06
1:8+20 wt% nano-HAp	2.17 ± 0.17
1:8+40 wt% nano-HAp	2.22 ± 0.06
1:8+60 wt% nano-HAp	2.39 ± 0.14

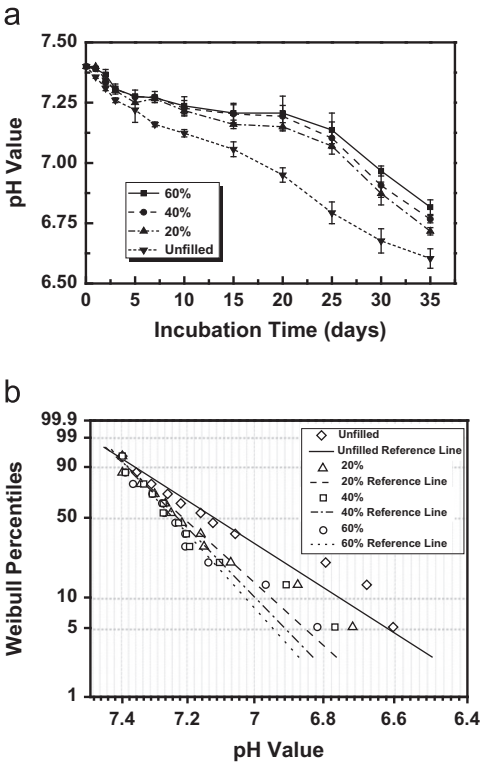

Fig. 9 – The pH changes of PBS after immersion of PDLLA scaffolds with 0, 20, 40, 60 wt% of nano-HAp, (a) pH versus incubation time and (b) the Weibull probability plot of pH value data.

The pH value of most body fluids ranges from 7.35 to 7.45 (Razaq, 2003), in which proteins and many other biological molecules can function properly. It is due to deviations in the pH value, for example, abnormal decrease or increase in blood pH, named acidosis and alkalosis can cause death if untreated (Starr and McMillan, 2012). Therefore, for bone tissue regeneration, it is of great importance to study the pH change of the aqueous medium when the scaffolds are used. Fig. 9(a) shows the pH evolution of PBS, for PDLLA scaffolds with different amounts of nano-HAp being immersed for 35 days. There is a decrease in the pH of the PBS after 35-day immersion of all the PDLLA scaffolds fabricated in this study. Such decrease in the pH is due to the carboxylic

acid produced from the degradation of the PDLLA via hydrolysis (Hile et al., 2004). The pH of the PBS containing unfilled PDLLA scaffolds decreases from the initial value of 7.4 to 6.6 after 35 days. Unlike the unfilled PDLLA scaffolds, the pH value changes of the PBS containing PDLLA/nano-HAp scaffolds exhibit different patterns and become stable during the incubation period from the 5th to the 20th days. Moreover, the pH values of the PBS containing different kinds of scaffolds fit the Weibull distribution as shown in Fig. 9(b). Fig. 9(b) shows decreasing trends in the pH value of all the PDLLA scaffolds and nano-HAp filled PDLLA scaffolds have a lower decreasing rate in the pH value than the unfilled one. The reason is that the nano-HAp has the effect of reducing the acidity of the medium (Schiller and Epple, 2003) and serves as a buffer system (Bucholz, 2002). Moreover, the more the nano-HAp is filled, the less the pH of the neighboring environment decreases. Therefore, the incorporation of the nano-HAp into the scaffolds might pave the way to control the pH value and avoid potential chronic inflammation complications during clinical applications.

4. Conclusions

PEG/Dex coated porous PDLLA/nano-HAp scaffolds, fabricated by a recently developed technique which combines coagulation, cold compression moulding, salt leaching and drug coating, showed improved bioactivity due to apatite formation, and enhanced mechanical properties close to human cancellous bone. The effects of the nano-HAp fillers on the molecular weight, mass loss and drug release behavior of the PDLLA scaffolds, as well as the pH value changes of PBS, were thoroughly investigated *in vitro*. Compared to the unfilled PDLLA scaffolds, incorporation of nano-HAp can slow down the polymer degradation and mass loss of the filled scaffolds, but cannot significantly affect the drug release rate. All the characteristics, such as the weight loss, degradation and apatite formation, had great effects on the mechanical properties of the scaffolds after incubation in the SBF. Results from the mechanical properties investigation show that the weight loss, polymer plasticization, and degradation of the PDLLA/nano-HAp scaffolds resulted in a reduction of their compressive moduli and strengths. On the other hand, compressive moduli and strengths of the scaffolds were improved due to the rigid apatite formation on them after the SBF incubation. Moreover, the PDLLA/nano-HAp scaffolds had a pH buffering effect during a 20-day incubation in the SBF, so that the risk of chronic inflammation complications can be reduced. The PEG/Dex coated porous PDLLA/nano-HAp scaffolds investigated in this study are suitable for bone repair applications.

Acknowledgments

The authors would like to thank the support from the Research Committee of The Hong Kong Polytechnic University (Project code: RU1A).

REFERENCES

Ang, K.C., Leong, K.F., Chua, C.K., Chandrasekaran, M., et al., 2006. Compressive properties and degradability of poly(e-caprolatone)/hydroxyapatite composites under accelerated hydrolytic degradation. Journal of Biomedical Materials Research. Part A 80a, 655–660.

Armentano, I., Dottori, M., Fortunati, E., Mattioli, S., Kenny, J.M., et al., 2010. Biodegradable polymer matrix nanocomposites for tissue engineering: a review. Polymer Degradation and Stability 95, 2126–2146.

Babensee, J.E., Anderson, J.M., McIntire, L.V., Mikos, A.G., et al., 1998. Host response to tissue engineered devices. Advanced Drug Delivery Reviews 33, 111–139.

Blaker, J.J., Nazhat, S.N., Maquet, V., Boccaccini, A.R., et al., 2011. Long-term in vitro degradation of PDLLA/Bioglass® bone scaffolds in acellular simulated body fluid. Acta Biomaterialia 7, 829–840.

Bucholz, R.W., et al., 2002. Nonallograft osteoconductive bone graft substitutes. Clinical Orthopaedics and Related Research 395, 44–52.

Chen, D.Z., Tang, C.Y., Chan, K.C., Tsui, C.P., Yu, P.H.F., Leung, M.C.P., Uskokovic, P.S., et al., 2007. Dynamic mechanical properties and in vitro bioactivity of PHBHV/HA nanocomposite. Composites Science and Technology 67, 1617–1626.

Chen, Y., Mak, A., Li, J., Wang, M., Shum, A., et al., 2005. Formation of apatite on poly(alpha-hydroxy acid) in an accelerated biomimetic process. Journal of Biomedical Materials Research. Part B, Applied Biomaterials 73B, 68–76.

Chen, L., Tang, C.Y., Chen, D.Z., Wong, C.T., Tsui, C.P., et al., 2011. Fabrication and characterization of poly-D-L-lactide/nano-hydroxyapatite composite scaffolds with poly (ethylene glycol) coating and dexamethasone releasing. Composites Science and Technology 71, 1842–1849.

Chou, Y., Chiou, W., Xu, Y., Dunn, J., Wu, B., et al., 2004. The effect of pH on the structural evolution of accelerated biomimetic apatite. Biomaterials 25, 5323–5331.

Deng, X.M., Hao, J.Y., Wang, C.S., et al., 2001. Preparation and mechanical properties of nanocomposites of poly(D,L-lactide) with ca-deficient hydroxyapatite nanocrystals. Biomaterials 22, 2867–2873.

Deng, C., Weng, J., Lu, X., Zhou, S.B., Wan, J.X., Qu, S.X., Feng, B., Li, X.H., et al., 2008. Preparation and in vitro bioactivity of poly (D,L-lactide) composite containing hydroxyapatite nanocrystals. Materials Science and Engineering: C 28, 1304–1310.

Deplaine, H., Ribelles, J.L.G., Ferrer, G.G., et al., 2010. Effect of the content of hydroxyapatite nanoparticles on the properties and bioactivity of poly(L-lactide)-hybrid membranes. Composites Science and Technology 70, 1805–1812.

Feng, K., Sun, H., Bradley, M.A., Dupler, E.J., Giannobile, W.V., Ma, P.X., et al., 2010. Novel antibacterial nanofibrous PLLA scaffolds. Journal of Controlled Release 146, 363–369.

Fu, S.Y., Feng, X.Q., Lauke, B., Mai, Y.W., et al., 2008. Effects of particle size, particle/matrix interface adhesion and particle loading on mechanical properties of particulate–polymer composites. Composites Part B: Engineering 39, 933–961.

Hile, D.D., Doherty, S.A., Trantolo, D.J., et al., 2004. Prediction of resorption rates for composite polylactide/hydroxylapatite internal fixation devices based on initial degradation profiles. Journal of Biomedical Materials Research 71B, 201–205.

Hutmacher, D.W., et al., 2001. Scaffold design and fabrication technologies for engineering tissues-state of the art and future perspectives. Journal of Biomaterials Science, Polymer Edition 12, 107–124.

Karageorgiou, V., Kaplan, D., et al., 2005. Porosity of 3D biornaterial scaffolds and osteogenesis. Biomaterials 26, 5474–5491.

Kokubo, T., Takadama, H., et al., 2006. How useful is SBF in predicting in vivo bone bioactivity?. Biomaterials 27, 2907–2915.

Kokubo, T., et al., 1991. Bioactive glass ceramics: properties and applications. Biomaterials 12, 155–163.

Kolan, K.C.R., Leu, M.C., Hilmas, G.E., Velez, M., et al., 2012. Effect of material, process parameters, and simulated body fluids on mechanical properties of 13-93 bioactive glass porous constructs made by selective laser sintering. Journal of the Mechanical Behavior of Biomedical Materials 13, 14–24.

Kovačevic, V., Vrsaljko, D., Blagojevic, S.L., Leskovac, M., et al., 2008. Adhesion parameters at the interface in nanoparticulate filled polymer systems. Polymer Engineering and Science 48, 1994–2002.

Langer, R., et al., 1998. Drug delivery and targeting. Nature 392, 5–10.

Liu, C., Xia, Z., Czernuszka, J.T., et al., 2007. Design and development of three-dimensional scaffolds for tissue engineering. Chemical Engineering Research and Design 85, 1051–1064.

Mourino, V., Boccaccini, A.R., et al., 2010. Bone tissue engineering therapeutics: controlled drug delivery in three-dimensional scaffolds. Journal of the Royal Society Interface 7, 209–227.

Oyane, A., Kim, H.M., Furuya, T., Kokubo, T., Miyazaki, T., Nakamura, T., et al., 2003. Preparation and assessment of revised simulated body fluids. Journal of Biomedical Materials Research Part A 65A, 188–195.

Razaq, S., et al., 2003. The effect of extracellular pH on matrix turnover by cells of the bovine nucleus pulposus. European Spine Journal 12, 341–349.

Rezwan, K., Chen, Q.Z., Blaker, J.J., Boccaccini, A.R., et al., 2006. Biodegradable and bioactive porous polymer/inorganic composite scaffolds for bone tissue engineering. Biomaterials 27, 3413–3431.

Schiller, C., Epple, M., et al., 2003. Carbonated calcium phosphates are suitable pH-stabilising fillers for biodegradable polyesters. Biomaterials 24, 2037–2043.

Sohier, J., Haan, R.E., De Groot, K., Bezemer, J.M., et al., 2003. A novel method to obtain protein release from porous polymer scaffolds: emulsion coating. Journal of Controlled Release 87, 57–68.

Song, W., Jun, Y., Han, Y., Hong, S., et al., 2004. Biomimetic apatite coatings on micro-arc oxidized titania. Biomaterials 25, 3341–3349.

Söntjens, S.H.M., Engels, T.A.P., Smit, T.H., Govaert, L.E., et al., 2012. Time-dependent failure of amorphous poly-D,L-lactide: influence of molecular weight. Journal of the Mechanical Behavior of Biomedical Materials 13, 69–77.

Starr, C., McMillan, B., et al., 2012. Human Biology, ninth ed. Yolanda Cossio, Belmont.

Tanahashi, M., Yao, T., Kokubo, T., Minoda, M., Miyamoto, T., et al., 1994. Apatite coating on organic polymers by a biomimetic process. Journal of the American Ceramic Society 77, 2805–2808.

Thomas, V., Jagani, S., Johnson, K., Jose, M.V., Dean, D.R., Vohra, Y.K., Nyairo, E., et al., 2006. Electrospun bioactive nanocomposite scaffolds of polycaprolactone and nanohydroxyapatite for bone tissue engineering. Journal of Nanoscience and Nanotechnology 6 (2), 487–493.

Wang, J., Wang, B.M., Schwendeman, S.P., et al., 2002. Characterization of the initial burst release of a model peptide from poly(D,L-lactide-co-glycolide) microspheres. Journal of Controlled Release 82, 289–307.

Wu, L.B., Ding, J.D., et al., 2004. In vitro degradation of three-dimensional porous poly(D,L-lactide-co-glycolide) scaffolds for tissue engineering. Biomaterials 25, 5821–5830.

Zhang, L.F., Sun, R., Xu, L., Du, J., Xiong, Z.C., Chen, H.C., Xiong, C.D., et al., 2008. Hydrophilic poly (ethylene glycol) coating on PDLLA/BCP bone scaffold for drug delivery and cell culture. Materials Science and Engineering C—Biomimetic and Suppramolecular Systems 28, 141–149.

Zheng, X., Zhou, S., Li, X., Weng, J., et al., 2006. Shape memory properties of poly(D,L-lactide)/hydroxyapatite composites. Biomaterials 27, 4288–4295.

Zhou, S.B., Zheng, X.T., Yu, X.J., Wang, J.X., Weng, J., Li, X.H., Feng, B., Yin, M., et al., 2007. Hydrogen bonding interaction of poly(D,L-lactide)/hydroxyapatite nanocomposites. Chemistry of Materials 19, 247–253.